DOE/PC/901

DOE/PC/90176--T54

DE92 004190

# FINAL TECHNICAL REPORT

September 1, 1990 through August 31, 1991

## PROJECT TITLE : CYCLONE REBURNING RETROFIT - CORROSION EVALUATION

DE-FG22-90PC90176

Principle Investigator: Hamid Sarv, Babcock and Wilcox
Other Investigator: Si-Cheng Kung, Babcock and Wilcox
Project Monitor: Dr. Ken Ho, CRSC

## ABSTRACT

Reduction of oxides of nitrogen ($NO_x$) from cyclone-equipped boilers is best accomplished by the application of reburning technology. Reburning process involves injection of a supplementary fuel above the cyclone to create a reducing zone for $NO_x$ removal. Overfire air is introduced above this zone to achieve complete combustion. Since the reburning zone must operate substoichiometrically, tube corrosion due to $H_2S$ formation within the modified combustion zones can be a potential concern when the reburning fuel is a high-sulfur coal. $H_2S$ is a corrosive gas and its concentration is an indicator of the tendency for fireside corrosion in fuel-rich combustion systems.

This research program was undertaken to assess corrosion resistance of three commercially available alloys (carbon steel, SA210-A1; low-alloy steel, SA213-T22; and stainless steel, SA213-TP304) as well as a coated steel alloy (SA213-T2). The surface chromium contents of the alloys ranged from 0 to 30%. Four air-cooled corrosion probes, each containing segments of the selected alloys were constructed. The probes were exposed for up to 1200 hours and at a metal temperature of 850°F to combustion gases generated by firing a high-sulfur Illinois #6 coal at conditions simulating coal reburning.

Corrosion rates of the tubular specimens were determined from changes in the wall thickness. Increasing the exposure time of the alloy samples increased the metal wastage, but decreased the corresponding rate. The corrosion rate also decreased with increasing chromium concentration in the alloys. Based on the results obtained in this study, the metal wastage rates of carbon and low alloy steels would be relatively high if substoichiometric combustion products are in direct contact with high temperature tubes in boiler waterwalls. A minimum of 16% Cr concentration is required to achieve a corrosion rate of less than 10 mpy (mil per year) based on 1200 hours of exposure. High Cr-containing materials like 304SS and the Cr/Si co- diffusion coating significantly improved the corrosion resistance and may be considered for replacing existing boiler tubes in areas of high $H_2S$ concentrations.

## DISCLAIMER

DISTRIBUTION OF THIS DOCUMENT IS UNLIMITED

(This project is funded by the U. S. Department of Energy as part of its cost-shared program with Illinois Department of Energy and Natural Resources.)

# EXECUTIVE SUMMARY

Reduction of $NO_x$ emissions by coal reburning is of commercial importance to cyclone boiler owners and the coal industry in the state of Illinois. Cyclone-equipped utilities in Illinois have over 7000 MW of electric generation capacity. Retrofitting these units with reburning technology provides economically favorable means for $NO_x$ control.

Since the reburning zone must be operated under sub-stoichiometric conditions, corrosion problems within this region are of prime concern. By operating the cyclone furnace with excess air, most (if not all) of the coal-sulfur oxidizes to $SO_2$. When coal reburning is employed for $NO_x$ reduction, $H_2S$ can also form in the reburning zone. $H_2S$ is a corrosive gas and its concentration is an indicator of the potential for fireside tube corrosion in fuel-rich combustion systems. Consequently, a research program was initiated to obtain information on tube corrosion rates under simulated reburning conditions.

A high-sulfur, Illinois #6 coal (Peabody) was burned with air at 120,000 Btu/hr in a stoker-fired furnace. Reburning zone stoichiometry, $H_2S$ levels, and the fluctuating boundaries between the reburning and overfire air zones, where reducing and oxidizing conditions alternate were simulated. Four air-cooled tubular probes representing waterwall tubes were placed in the furnace and their metal temperature was maintained at 850°F. Each corrosion specimen contained eight segments constructed of four different materials (two segments per material) including carbon steel, low alloy steel, stainless steel, and a coated steel. Chromium content of the selected alloys ranged from 0 to 30%. Three probes were positioned in the reducing environment while the fourth was placed above the overfire air port where excess air mixed with reburning zone products. Probe corrosion rates were determined from thickness reductions for specimens recovered after 400, 800, and 1200 hours of exposure to combustion gases.

In general, metal wastage of the alloys in the simulated reburning zone increased with increasing exposure time, while the corresponding rates decreased with time. The corrosion rate was low for the high chromium content alloys. One should note that the maximum waterwall temperature that may be experienced in once-through, forced circulation, supercritical boilers was sustained in this work. Other boilers (e.g., natural circulation radian type) experience lower tube wall temperatures, typically around 650-750°F. Since corrosion rate is a strong function of temperature, the corrosion attack at 850°F is expected to be most severe and, therefore, should represent the worst case.

Optimized reburning burner design also prevents tube corrosion by avoiding flame impingement on boiler walls, and confining the $NO_x$ reducing zone to the boiler center. Low chromium content carbon or low-alloy steels can be protected by commercial chromium coating processes.

## 1.0 OBJECTIVES

Carbon steel tubes are commonly used in the waterwall construction of cyclone-fired utility boilers. Currently, very little information is available on long-term tube corrosion assessment in cyclone/reburning applications. This research program was undertaken with the following primary objectives:

- To evaluate wastage of carbon steel tubes used in cyclone boilers, and their suitability in coal reburning retrofits for $NO_x$ control.
- To identify alternative and cost effective alloy(s), if the extent of corrosion with existing carbon steel tubes is proven to be unacceptable.

In order to accomplish these objectives, the research plan was organized as five main tasks:

Task I : Test Plan and Site Preparation
Task II : Combustion Simulation
Task III : Corrosion Testing
Task IV : Data Analysis
Task V : Management and Reporting

Each task was divided into a number of sub-tasks. A detailed outline of the project tasks and subtasks was given in the first quarterly report.

## 2.0 INTRODUCTION AND BACKGROUND

### 2.1 $NO_x$ Reduction by Reburning

Reburning is a proven $NO_x$ reducing technology which offers cyclone boiler owners a promising alternative to the more expensive flue gas cleanup techniques. The reburning process employs multiple combustion zones in the furnace. Locally reducing conditions for conversion of $NO_x$ to $N_2$ are created by introducing a supplementary fuel/air mixture above the main combustion zone. Excess air penetrates through the overfire air ports into the furnace above the reburning zone to complete the oxidation of combustibles. Figure 2.1 shows the different combustion zones in a reburning arrangement. Between 50-70% $NO_x$ removal was demonstrated previously [1] at a 6 MBtu/hr pilot-scale, Small Boiler Simulator facility when cyclone firing and coal reburning were combined. In the same study, a maximum $H_2S$ concentration of 300 PPMV was measured between the two parallel reburn burner flames while firing Illinois #6 (Peabody) coal. $H_2S$ levels were less than 20 PPMV near the sidewalls, and oxidized rapidly to $SO_2$ in the burnout zone. Since $H_2S$ is a corrosive gas, it may pose a potential problem and concern in reburning retrofits using high-sulfur Illinois coals [2].

### 2.2 Combustion-Induced Corrosion

Chemical equilibrium calculations indicate that fuel-sulfur can evolve in different forms during combustion. Under oxidizing conditions, such as in the cyclone barrel and burn-out zone, sulfur reacts predominately with oxygen to form $SO_2$ and $SO_3$. In a reducing or substoichiometric combustion environment, fuel-sulfur is primarily converted to $H_2S$. $H_2S$ concentration is a good indication of the gas corrosivity. B&W's bench-scale test data [4] have proven that the corrosion rates of alloys indeed increase with increasing $H_2S$ concentration in the flue gas.

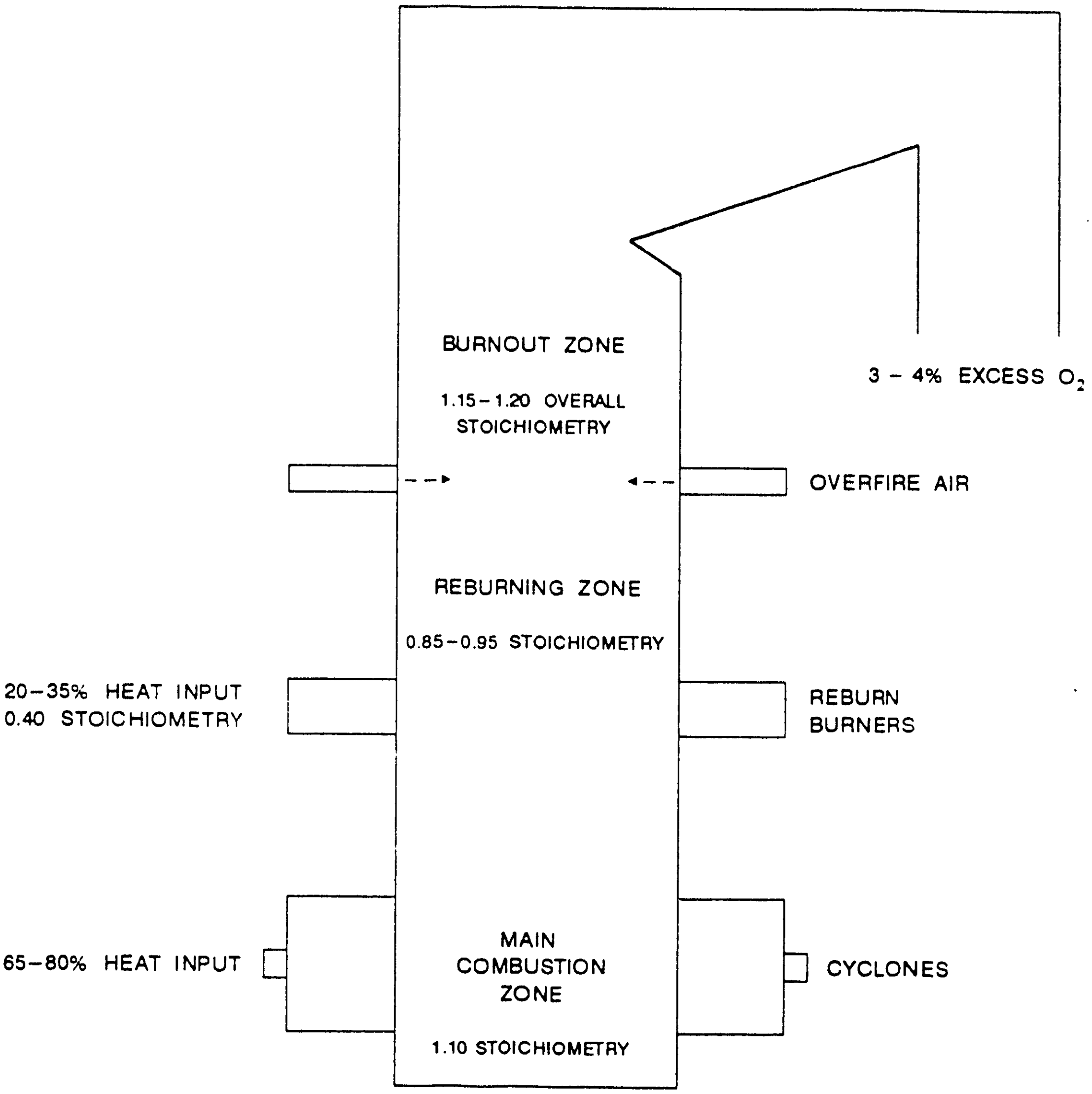

FIGURE 2.1. $NO_x$ control by coal reburning

Substoichiometric combustion of sulfur-containing fuels greatly hinders the ability of alloys to form oxide scales on tube surfaces while enhancing the formation of sulfides. In general, the growth rate (equivalent to corrosion rate) of sulfides is a few orders of magnitude higher than that of oxides. In addition, many oxides are considered protective once formed on the alloy surface, but none of the sulfides are known to be protective. As a result, the corrosion rates (or metal wastage) in the reburning zone will increase if sulfides are allowed to form on the tube surface.

Limited corrosion data are available from bench-scale experiments in excessively high $H_2S$ concentration environments (5,000 to 20,000 ppm). Because a direct relationship between the corrosion rate and $H_2S$ concentration is still lacking at the present time (although work is being done at B&W as part of a separate program to complete the correlation), it is impractical to extrapolate the corrosion rate to $H_2S$ levels found typically in coal-fired facilities.

There is also some evidence [5] that corrosion rates of alloys placed in alternating reducing/oxidizing environments are noticeably higher than those exposed constantly to a reducing atmosphere. Such conditions may exist at the boundary of the reburning and the burn-out zones, as well as between the reburning and the primary combustion zones. Fluctuations in the flue-gas composition can change the corrosion products on the metal surfaces interminably between sulfides and oxides [4]. Because of the density difference and the associated volume changes, more voids and cracks could form in the corrosion products (or scales). As a result, the scales become even less protective, and a more pronounced corrosion attack can occur. These concerns were subjects of the present investigation.

## 3.0 EXPERIMENTAL FACILITY AND PROCEDURES

### 3.1 Combustion Facility

Figure 3.1 shows a schematic of the refractory-lined, stoker-fired furnace. This unit is capable of burning stoker-grade coal (<1 inch with up to 15% fines), wood pellets, and other solid fuels. A variable-speed, calibrated screw feeder supplies the fuel to the bottom of the 1 $m^3$ (35 $ft^3$) stoker chamber. A forced draft fan provides the primary combustion air which enters the furnace through tuyers surrounding the burner. Overfire air is introduced through two diametrically opposed ports at 13 feet above the stoker furnace. The furnace bottom is sealed with water contained in a tank. Combustion generated ash and molten slag are removed after falling into the water tank. A wall-fired auxiliary gas burner is used to initiate solid fuel combustion and to increase the gas temperature.

A drawing of the burner rig is shown in Figure 3.2. Several viewing and access ports are situated along the connecting stack sections. Four of these ports accommodate the air-cooled corrosion probes. In this work, three probes were positioned in the reducing zone at 7.5, 25.5, and 43.5 inches above the furnace roof. The forth probe was placed 6 inches higher than the overfire air ports to simulate alternating oxidizing/ reducing boundaries. Air flow rates, stoichiometries, and other pertinent information were determined by post processing and analysis of the data collected from orifice meters, rotameters, pressure gauges, thermocouples, etc.

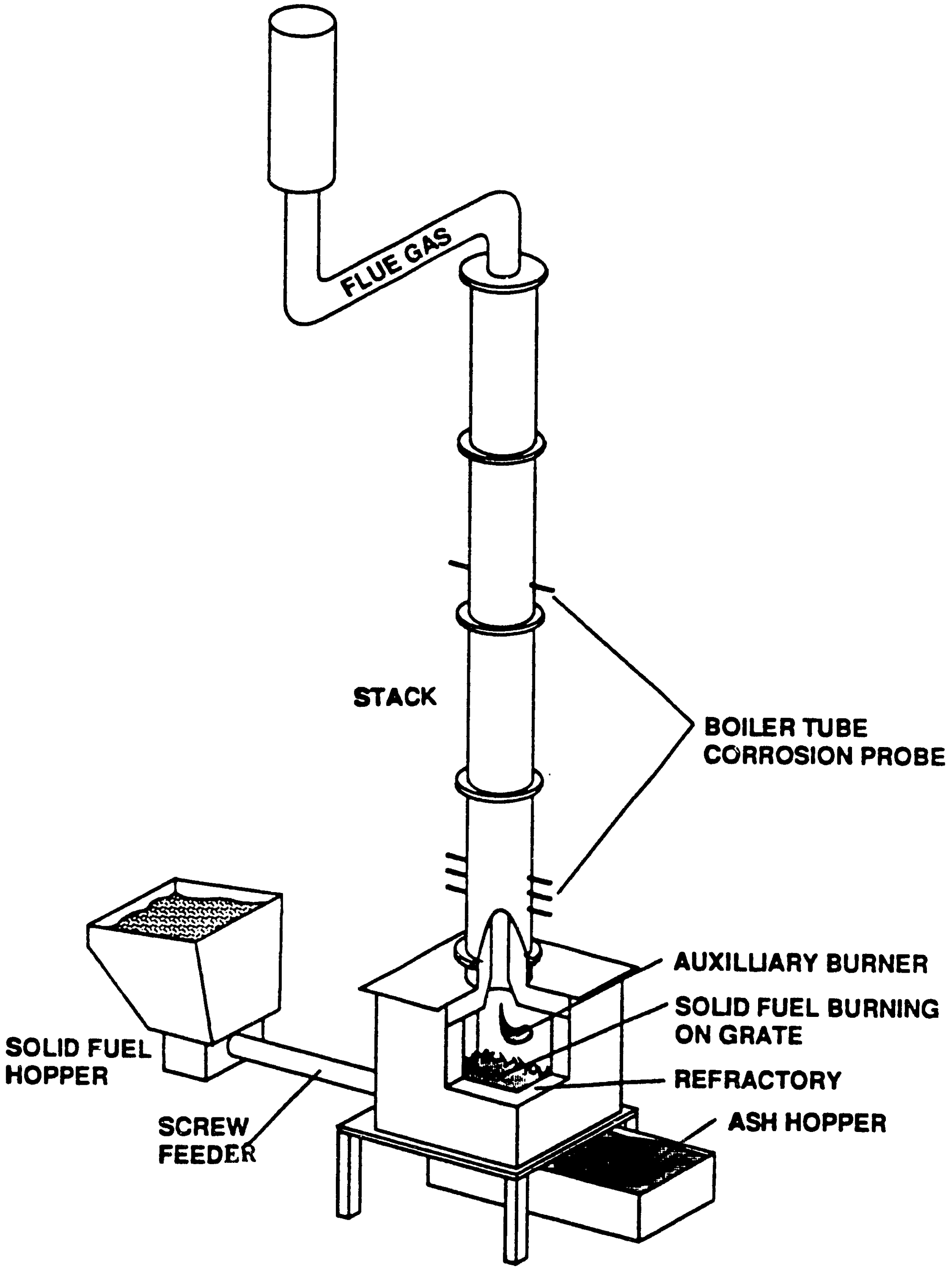

FIGURE 3.1. Overall schematic of the combustion facility

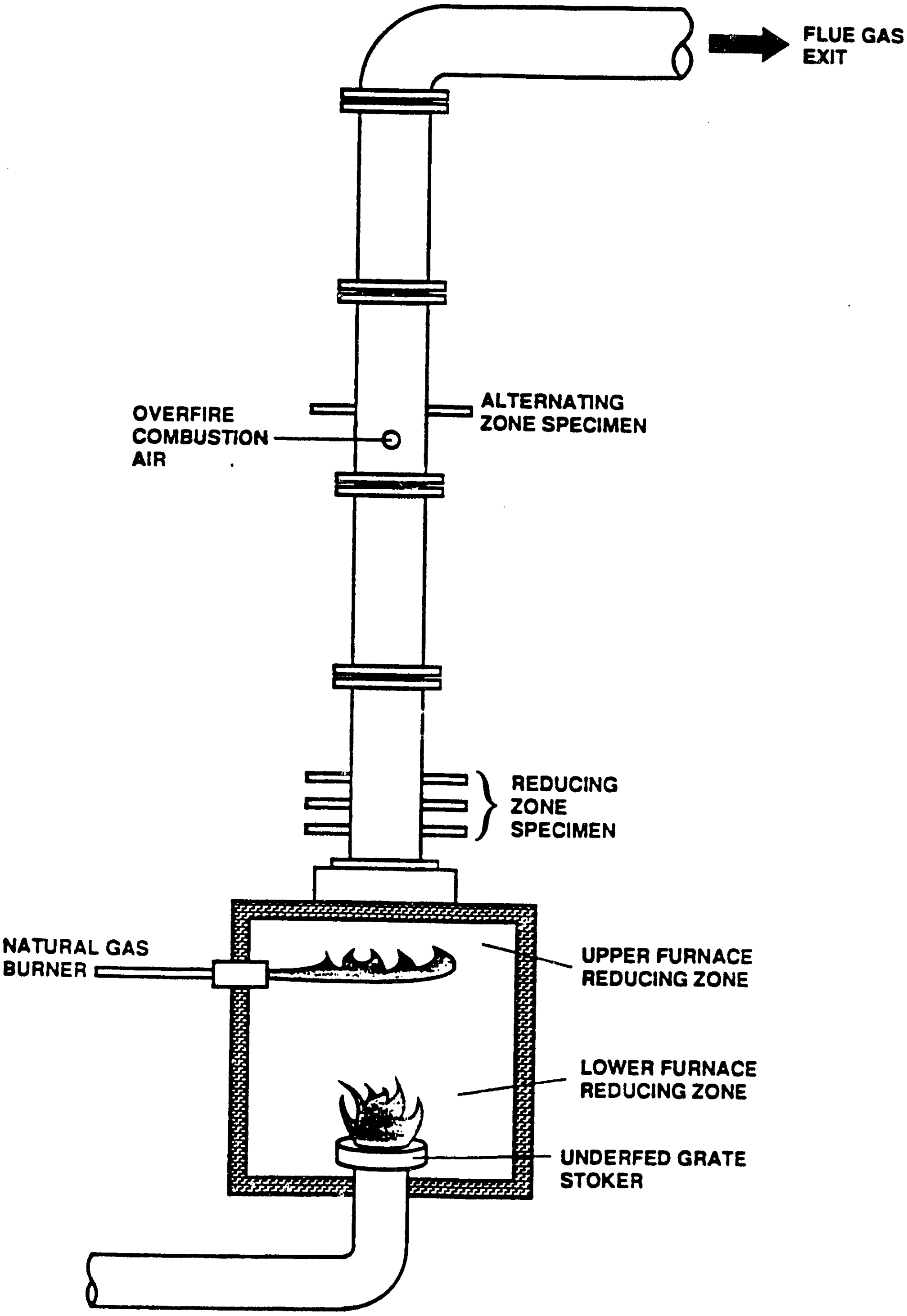

FIGURE 3.2. Schematic of the stoker-fired furnace

## 3.2 Gas Sampling and Analysis System

Gas species measurements were limited to $O_2$, $SO_2$, and $H_2S$ concentrations. Table 3.1 lists the gas analyzers and their measurement principles. Stack gases were sampled continuously at 3 feet above the oxidizing/reducing probe. After filtering and drying, $O_2$ and $SO_2$ concentrations were measured and recorded. Both analyzers were calibrated with certified gas standards.

For $H_2S$ measurements, a slip stream was withdrawn from the stack via a vacuum pump through a ceramic tube as shown in Figure 3.3. A hand-operated bellows pump pulled 100 $cm^3$ of the gas with each stroke into a $H_2S$ detector Dräger™ tube [5], inserted in a tee fitting. Each tube contained either $Cu^{2+}$, $Pb^{2+}$, or Hg compounds which react selectively with $H_2S$ to form a brown sulfide. Actual concentrations were based on the discolored length of the filling material inside the scaled glass tube and the number of suction strokes. Although calibration is inherent to the design of Dräger tubes, measured concentrations relative to a 152 PPMV $H_2S$ standard were 1.3 to 34.2% less. The deviation is attributable to systematic errors.

## 3.3 Alloy Selection

The corrosion resistance of alloys can vary significantly with their chemical compositions. Under a corrosive environment, metals will react with the corrosive species to form various corrosion products. At high temperatures, these products are thick enough to be termed as scales. After having formed on the alloy surfaces, some scales can serve as diffusion barriers to slow down the reaction kinetics and in turn lower the corrosion rates. These scales are beneficial for the alloys and therefore are considered protective. For others, the scales cannot serve effectively as diffusion barriers and thus are not protective. For example, both chromium and iron can react with oxygen to form chromium oxide ($Cr_2O_3$) and iron oxides ($FeO_{1-x}$, $Fe_3O_4$, and $Fe_2O_3$), respectively. However, chromia scales are known to act as an effective barrier layer on metals and slow down the oxidation process at high temperatures, but iron oxides do not. When both elements co-exist in an alloy, the corrosion resistance of the alloy is essentially equivalent to its ability of forming chromia on the alloy surface. General discussions on corrosion mechanisms have been given elsewhere [6].

Carbon and low-alloy steels are commonly used in utility boilers for various applications. However, under severe environments, improved corrosion resistance of boiler parts may be required and is usually achieved by replacing the component material with chromia-forming steels. Nonetheless, use of these steels is often more costly. To guarantee the formation of the protective chromia scales in a given corrosive environment, useful alloys must have a minimum chromium concentration. In general, the required Cr content for an alloy decreases as conditions change from reducing to oxidizing. In the presence of $H_2S$, the corrosion rate is expected to be more severe, and the required Cr concentration in the alloy will be higher. It is therefore imperative to examine the effect of Cr content on the materials performance in substoichiometric combustion environments.

Three tubing alloys and a special coating were selected. They included carbon steel SA210-A1, low-alloy steel SA213-T22, stainless steel SA213-TP304, and Cr/Si co-diffusion coated SA213-T2. Carbon steel contains essentially no chromium; therefore, no chromia is expected to form on the surface. Alloy T22 contains ~2.25% Cr (still not a chromia former) and is a commonly used waterwall material. Stainless steel 304 has a nominal 18% Cr and is known to be a chromia-forming alloy under most corrosive conditions. The high-temperature Cr/Si diffusion coating was developed by the Ohio State University Materials Engineering Department, using a unique pack cementation process. Alloy T2, with an original Cr concentration of ~0.5%, was used as the

TABLE 3.1. Gas Analysis Instrumentation

| Gas Species | Analyzer | Model Number | Measurement Principle |
|---|---|---|---|
| $O_2$ | Teledyne | 326RB | Polarographic |
| SO | Teledyne | 691C | UV Absorption |
| $H_2S$ | Drager Tube | 67 33151 | Reaction with $Cu^{2+}$ |
| $H_2S$ | Drager Tube | CH 29101 | Reaction with $Pb^{2+}$ |
| $H_2S$ | Drager Tube | 67 28821 | Reaction with Hg |

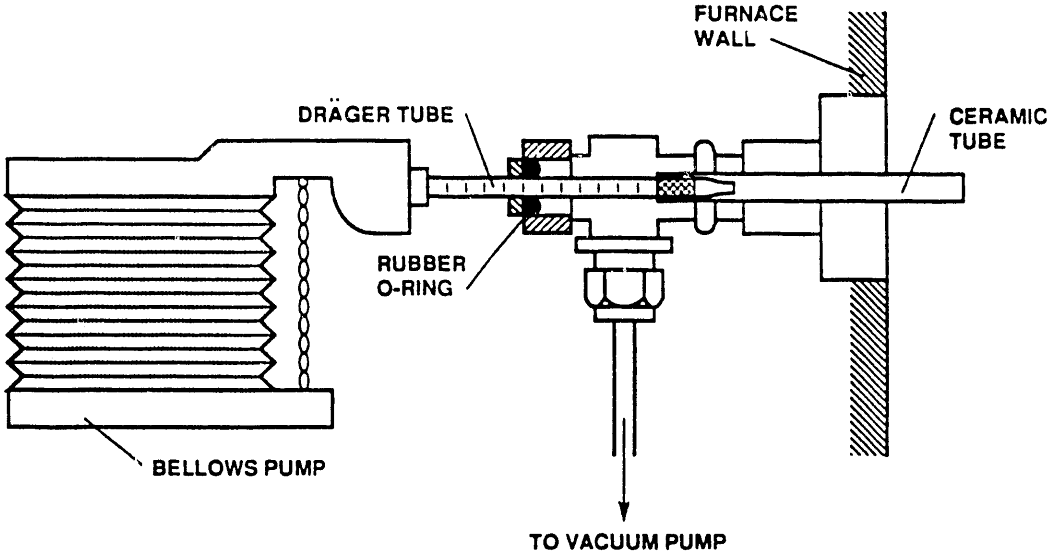

FIGURE 3.3. $H_2S$ sampling and measurement system

substrates. After coating, the resulting surface composition on the T2 substrates became ~30% Cr 3% Si, and a balance of Fe. Selection of these alloys spanned the Cr concentration in this investigation from 0 to 30%. Table 3.2 summarizes the chemical compositions of the selected alloys.

TABLE 3.2. Chemical Compositions of the Selected Alloys

| Alloy | Grade | C | Mn | P | S | Si | Cr | Mo | Ni | Fe |
|---|---|---|---|---|---|---|---|---|---|---|
| 1 | SA210-A1 | 0.16 | 0.71 | 0.026 | 0.025 | 0.28 | -- | -- | -- | bal |
| 2 | SA213-T22 | 0.12 | 0.42 | 0.012 | 0.028 | 0.30 | 2.30 | 0.96 | 0.16 | bal |
| 3 | SA213-TP304 | 0.045 | 1.74 | 0.025 | 0.025 | 0.42 | 18.27 | -- | 9.50 | bal |
| 4 | Cr/Si-coated SA-213-T2 (at surface) | -- | -- | -- | -- | 3.00 | 30.00 | -- | -- | bal |

## 3.4 Design of Corrosion Probes

All four tubing alloys were machined into tube segments. Each segment was 1" OD x 1.0625" long with a wall thickness of 0.088 ± 0.001". The end of each segment was shaped to contain extruded and indented chamfers at 10° and 45°, respectively. The chamfers allowed multiple segments of different samples to be connected in series on each probe and eliminated leakage of the cooling air. High-temperature diffusion coating was applied to the outside and inside surfaces of the T2 sample segments. Because the coating introduced additional mass uniformly into the substrates via diffusion processes, the resulting wall thickness of the coated T2 segments became 0.090 ± 0.001" (i.e., each side gained 0.001").

All corrosion probes consisted of eight tube segments with duplicate samples for each alloy. Figure 3.4 illustrates the arrangement of three chamfered tube segments. Pressure was applied at both ends of the probes to achieve a tight fit between the samples. Figure 3.5 shows a photograph of a completely assembled corrosion probe prior to mounting in the furnace. Tube segments of the same material on each probe were separated by other alloys. Figure 3.6 identifies the sample arrangement of the four corrosion probes and their exposure times. The relative flue-gas flow direction is also shown in Figure 3.6.

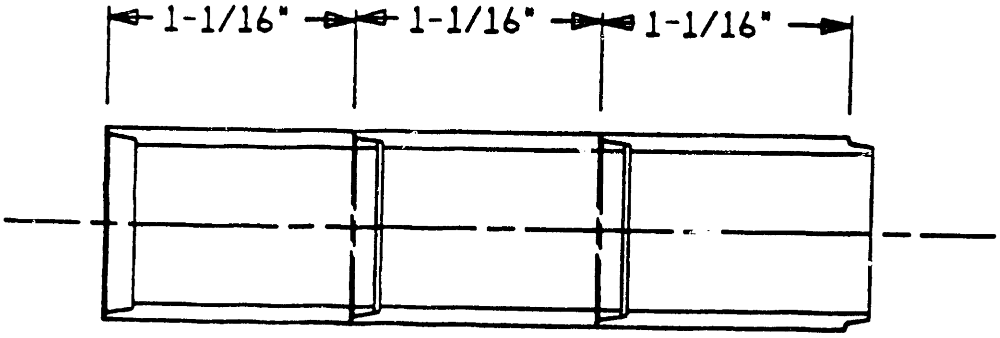

FIGURE 3.4. Arrangement of the chamfered tube segments

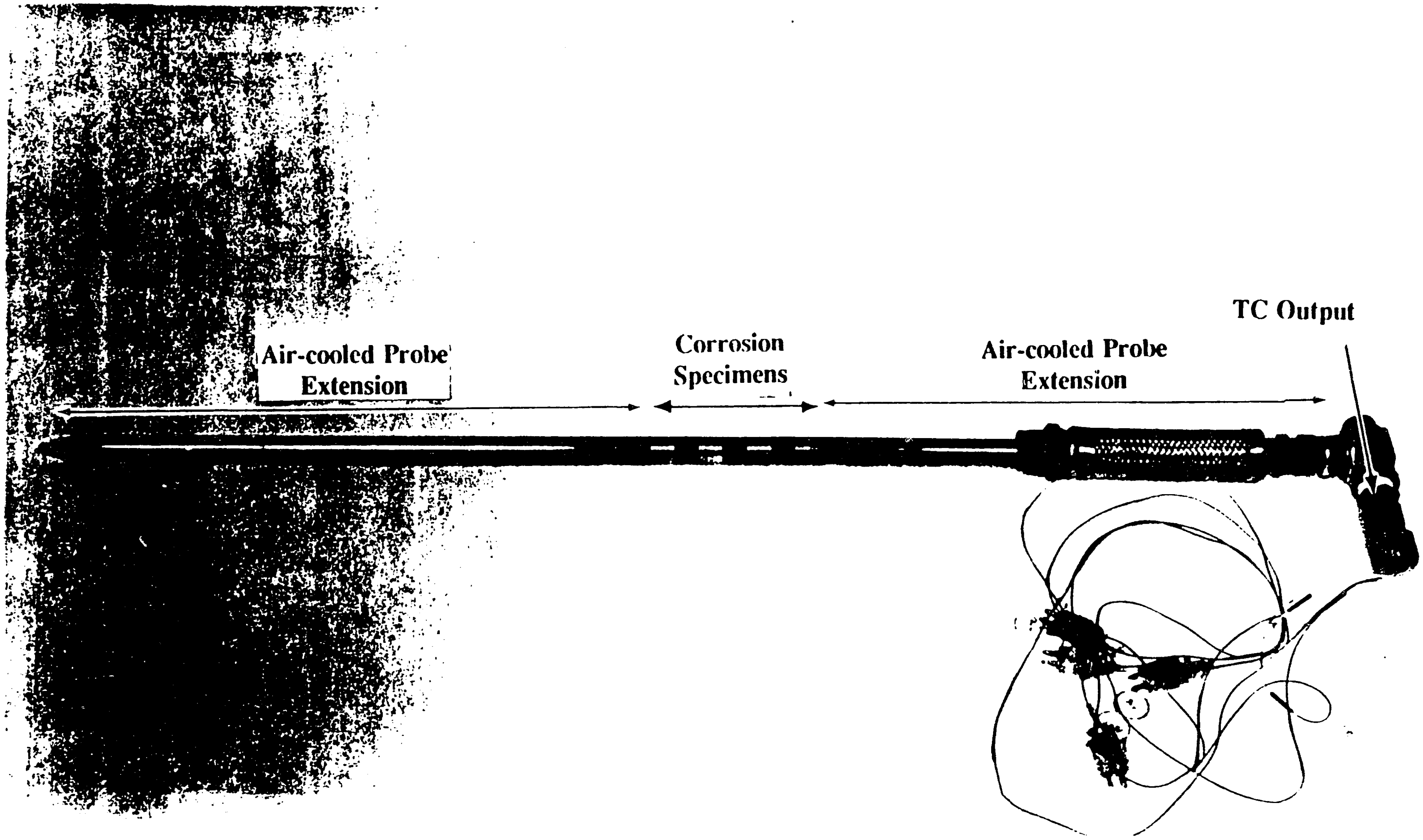

Figure 3.5. Photograph of an assembled corrosion probe before installation in the combustion facility

| | | | | | | | |
|---|---|---|---|---|---|---|---|
| Cr/Si | T22 | 304 | A1 | Cr/Si | T22 | 304 | A1 |
| TC | | TC-control | | | TC | | TC |

**Probe #2** - 800-hour lower probe

| | | | | | | | |
|---|---|---|---|---|---|---|---|
| T22 | 304 | A1 | Cr/Si | T22 | 304 | A1 | Cr/Si |
| TC | | TC | | TC | | | TC |

**Probe #3** - 1200-hour lower probe

| | | | | | | | |
|---|---|---|---|---|---|---|---|
| 304 | A1 | Cr/Si | T22 | 304 | A1 | T22 | Cr/Si |
| TC | | | TC-control | | TC | | TC |

**Probe #4** - 400-hour lower probe

| | | | | | | | |
|---|---|---|---|---|---|---|---|
| 304 | Cr/Si | T22 | A1 | 304 | Cr/Si | T22 | A1 |
| TC | | | | TC | TC | | TC |

← Cooling-Air Flow Direction

↑
Flue-Gas Flow Direction

**FIGURE 3.6. Sample arrangement of the corrosion probes**

Four Type-K thermocouples (TC) were tig-welded to four sample segments on each probe. The weld was made into pre-drilled holes on the inner surfaces of the tube samples. TC junctions were partially embedded into the tube walls.

Compressed air at room-temperature was supplied continuously through the corrosion probes to maintain a metal temperature of 850°F. The direction of air flow was from right to left as illustrated in Figure 3.6. The flow rates were controlled electronically based on signals from selected thermocouples inside the probes (labeled TC - control in Figure 3.6). Total air supply to the lower three probes was adjusted by one main flow controller and distributed through different valves. The upper probe temperature was controlled independent of the other probes. It is important to note that the maximum waterwall temperature that may be experienced in once-through, forced circulating supercritical boilers is about 850°F. Since corrosion rate is a strong function of temperature, the corrosion attack at 850°F is expected to be most severe and, therefore, should represent the worst case. Typical tube temperatures for other boilers (e.g., natural circulating radiant type) are within 650 to 750°F, and the expected corrosion rates are substantially lower.

# 4.0 RESULTS AND DISCUSSION

## 4.1 Coal Analysis

Proximate, ultimate, and heating value analyses were performed on an as-received Illinois #6 (Peabody) coal sample according to standard ASTM procedures. Those results are given in Table 4.1.

**TABLE 4.1. Ultimate, Proximate, and Heating Value Analyses for Illinois #6 (Peabody) Coal**

| Basis | Constituents | Composition (Weight %) |
|---|---|---|
| As-received | Carbon | 58.13 |
| | Hydrogen | 4.26 |
| | Nitrogen | 1.13 |
| | Sulfur | 3.54 |
| | Oxygen | 6.70 |
| | Moisture | 16.39 |
| | Ash | 9.85 |
| | | ------ |
| HHV = 10212 Btu/lb | Total | 100.00 |
| | Volatile Matter | 36.78 |
| | Fixed Carbon | 36.98 |

## 4.2 Coal Reburning Simulation

Combustion simulation experiments were conducted to establish the operating parameters that simulate coal reburning conditions (stoichiometry and $H_2S$ levels). Overall heat release from burning coal and natural gas was 120,000 Btu/hr. Combustion of natural gas accounted for about 16% of the total heat input. Centerline gas temperatures in the vicinity of the lower and upper furnace corrosion probes averaged at 2319 and 1030°F, respectively.

Figure 4.1 shows the effect of reburning zone stoichiometry on $H_2S$ concentration. As expected, $H_2S$ levels increase with decreasing stoichiometry. At or near stoichiometric conditions, little or no $H_2S$ was detected as coal-S transformed quantitatively to $SO_2$. In this program, the $H_2S$ concentration was maintained around 200 PPMV, corresponding to a reducing zone stoichiometric ratio of 0.9. For a stack $O_2$ level of 2.5%, $SO_2$ concentrations were 2600 PPMV.

## 4.3 Probe Temperature Profiles

Figure 4.2 summarizes the average temperature profiles along the corrosion probes. Segments 1 and 8 correspond to samples located at the cooling-air exit and inlet, respectively. These temperature profiles exhibit a maximum near the center of the probes. As expected, tube segments nearest to the cooling air inlet (i.e., the right-hand side in Figures 3.6 and 4.2) experienced rapid quenching and, thus, had the lowest temperature readings. Towards the middle, the air became heated, leading to higher metal temperatures as well. Temperature also dropped near the probes exits due to heat loss to stack walls.

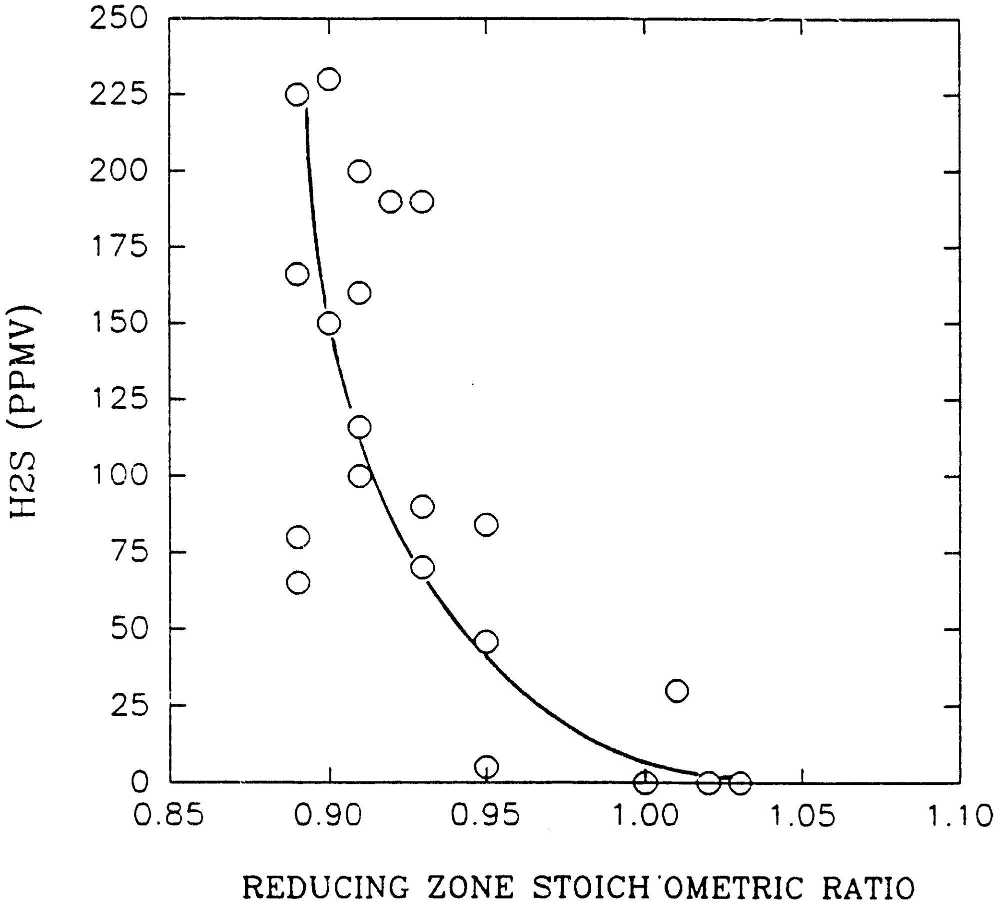

FIGURE 4.1. Effect of stoichiometry on $H_2S$ formation for the combustion of Illinois #6 (Peabody) Coal with air

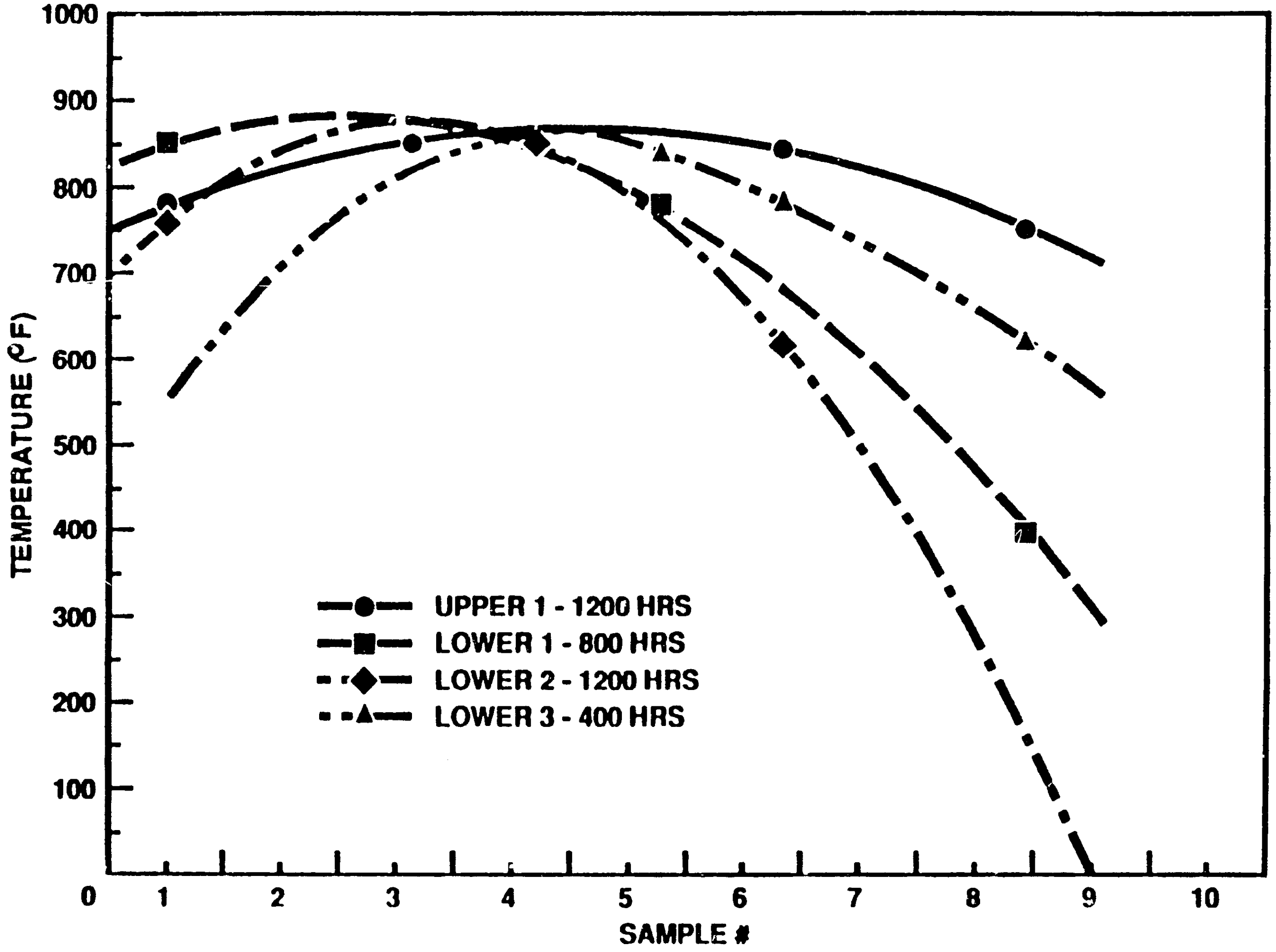

4.2. Temperature profiles of the corrosion probes

Only segments 2-5 (shaded in Figure 3.6) fell in the 750-850°F temperature range. These segments were carefully removed from the exposed probes for subsequent analyses. Generally, these samples were covered with a thick layer of ash deposit. During the probe disassembly, the ash deposit and the underlying corrosion products (scales) had a tendency to break away and spall off from the tube surfaces.

## 4.4 Corrosion Rate Determination

In principle, corrosion rates can be calculated by relating changes in the wall thickness to the exposure time. Conventionally, the remaining wall thickness is measured with a micrometer, after dissolving the surface products (both the deposit and scale) in acidic solutions. However, this technique involves a high degree of uncertainty because thorough dissolution of the corrosion products in acids is difficult. In particular, there is no reliable device to detect the surface cleanliness, making the dissolution processes heavily reliant upon human inspection. If the surface products are not completely cleaned, the apparent thickness will be more than what it actually is. Conversely, if the sample is over-cleaned the acidic solution will attack the tube metal and result in an excessive corrosion rate. The additional error could cause a deviation of more than ±0.001", which is equivalent to the tube-segment machining tolerance.

For better accuracy, in this study, the remaining wall thicknesses were determined via the cross-sectional microscopic technique. Because the sample segments were chamfered at both ends, they were first cross-sectioned near the center. One piece from each sample was then mounted in bakelite and metallographically finished to reveal the cut surface. During the metallography preparations, water was not used to preserve any water-soluble products existing on the sample surfaces. The remaining wall thicknesses were then measured using a Nikon optical microscope (Nikon Measurescope, Model 20). This microscope is capable of measuring to within ±0.0001".

The remaining wall thicknesses on both the leading and trailing edges of each sample were measured. The leading edge is defined as the side directly facing the flue-gas flow direction, and the trailing edge is 180° away from the leading edge. Tables 4.2 - 4.5 list the wall-thickness variations of the four alloys. The measurements have been rounded up to the nearest mil (1 mil

**TABLE 4.2. Wall Thickness Measurements of Lower-Probe Samples (in mil) After 400 Hours**

| | | Leading Edge | | Trailing Edge | |
|---|---|---|---|---|---|
| Alloy | $t_o$ | t | Δt | t | Δt |
| 210A1 | 88 | 86 | -2 | 86 | -2 |
| T22 | 88 | 87 | -1 | 86 | -2 |
| 304SS | 88 | 87 | -1 | 87 | -1 |
| Cr-Si/T2 | 90 | 91 | 0 | 91 | 0 |

**Note**:

$t_o$ - Initial wall thickness
t - Final wall thickness
Δt - Wall thickness change

= 0.001"). Again, the three lower probes were located in a region simulating the reburning zone, and the upper probe was in the reducing/oxidizing environment anticipated at boundaries above and below the actual reburning zone.

TABLE 4.3. Wall Thickness Measurements of Lower-Probe Samples (in mil) After 800 Hours

| | | Leading Edge | | Trailing Edge | |
|---|---|---|---|---|---|
| Alloy | $t_o$ | t | Δt | t | Δt |
| 210A1 | 88 | 85 | -3 | 84 | -4 |
| T22 | 88 | 86 | -2 | 86 | -2 |
| 304SS | 88 | 87 | -1 | 88 | 0 |
| Cr-Si/T2 | 90 | 88 | -2 | 89 | -1 |

TABLE 4.4. Wall Thickness Measurements of Lower-Probe Samples (in mil) After 1200 Hours

| | | Leading Edge | | Trailing Edge | |
|---|---|---|---|---|---|
| Alloy | $t_o$ | t | Δt | t | Δt |
| 210A1 | 88 | 83 | -5 | 83 | -5 |
| T22 | 88 | 84 | -4 | 85 | -3 |
| 304SS | 88 | 87 | -1 | 87 | -1 |
| Cr-Si/T2 | 90 | 91 | 0 | 91 | 0 |

TABLE 4.5. Wall Thickness Measurements of Upper-Probe Samples (in mil) After 800 Hours

| | | Leading Edge | | Trailing Edge | |
|---|---|---|---|---|---|
| Alloy | $t_o$ | t | Δt | t | Δt |
| 210A1 | 88 | 82 | -6 | 83 | -5 |
| T22 | 88 | 85 | -3 | 85 | -3 |
| 304SS | 88 | 87 | -1 | 87 | -1 |
| Cr-Si/T2 | 90 | 91 | 0 | 90 | 0 |

The wall-thickness reduction data in Tables 4.2 - 4.4 for the lower probes were used to plot the best-fit curves in Figure 4.3 as a function of time. The solid lines represent the variation of metal wastage on the leading edges and dashed lines are for the trailing edges. The difference in the metal wastages between the trailing edge and the leading edge for each material is, in general, quite small and is within the experimental error. A small difference in the corrosion attack indicates that the corrosive environment in the burner rig on both edges of the probes was similar, i.e., the environment was not significantly affected by the flow pattern around the radius of the probes. As expected, the wall-thickness loss of the alloys increased with time. The carbon steel has the highest metal wastage, followed by T22 and 304SS. The Cr/Si-coated T2 shows the least change in the wall thickness with time or the greatest corrosion resistance among the four materials.

Corrosion rates have been expressed in a variety of ways in the literature [7]. In theory, slopes of the curves in Figure 4.3 at a given time are equivalent to the instantaneous corrosion rates. Therefore, the corrosion rates of these materials actually decreased with time, as indicated by the decreasing slopes in the plot. However, direct extraction of the corrosion rate data from the slopes requires a better resolution or more data points to establish representative trends. Alternatively, the corrosion mechanisms must be fully understood. In the absence of detailed information on corrosion reactions, curves with a high degree of accuracy can only be constructed by conducting numerous long-term experiments. From an engineering standpoint, this is not practical. Therefore, the linearized corrosion rate is often extrapolated to one year and expressed in mil per year (mpy). Although this approach was also used in this work, it does not reflect the true corrosion rates. Instead, it provides a basis for comparing different alloys for selection, so long as they have been treated to similar conditions.

Figure 4.4 compares the corrosion rates as a function of chromium concentration in the alloys. Best-fit curves for the corrosion rates of the three lower probes are plotted using the calculated results based on the method described above. It is apparent that the corrosion rate decreases rapidly with increasing chromium content. Furthermore, the corrosion rate for each alloy (or a fixed Cr%) decreases with increasing exposure time. These observations agree well with the expected performance of metallic materials because (1) a higher Cr% promotes the formation of protective chromia scale and (2) the thicker the scale, the more effective diffusion barrier it provides, i.e., the slower the corrosion process. As seen in Figure 4.4, the measured corrosion rates of carbon and low-alloy steels are within 20-50 mpy; for the stainless steel and high-chromium coated steel the range is 0-20 mpy. In either case, the lower limit corresponds

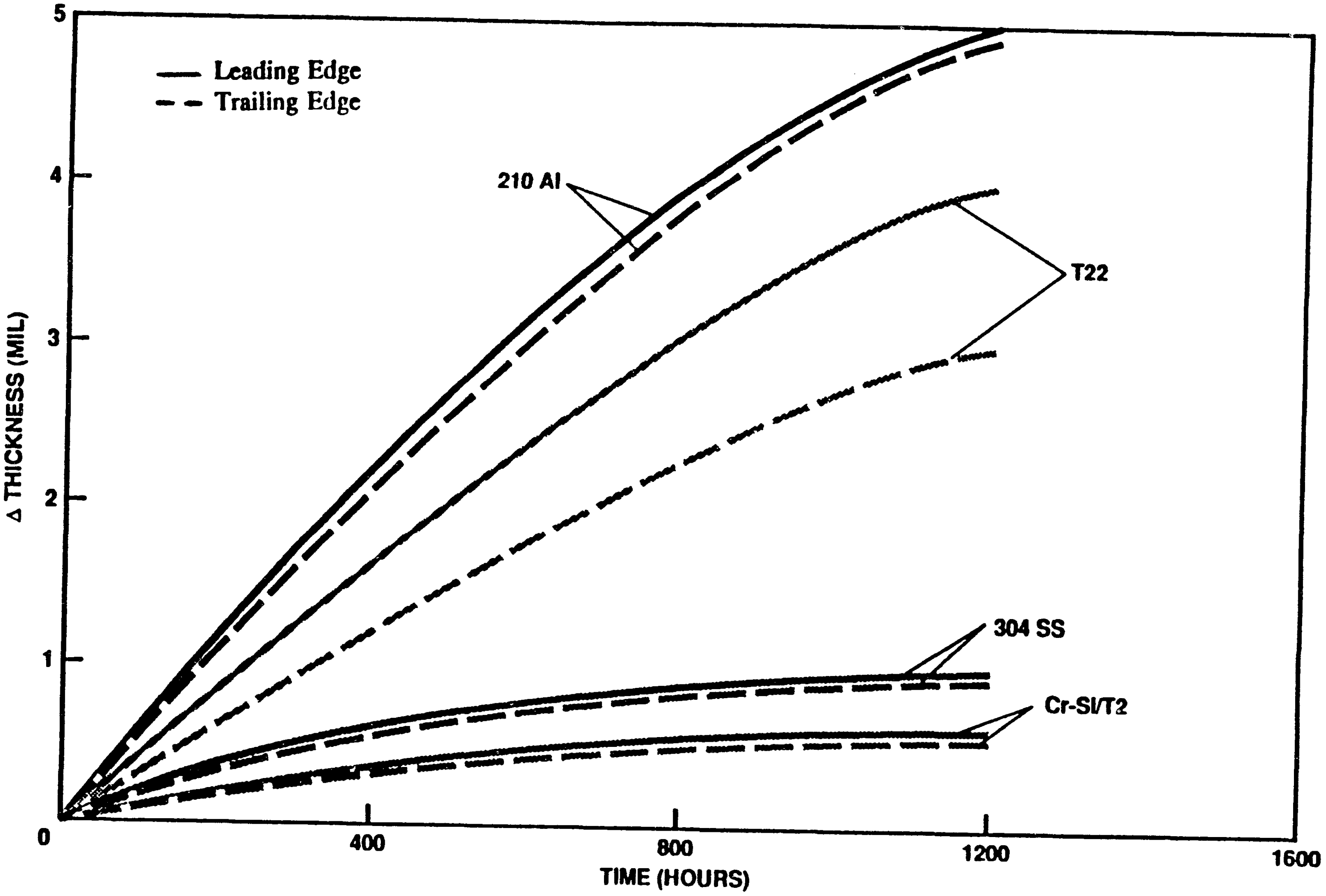

Figure 4.3. Effect of exposure time on metal wastage for alloys at 750-850°F

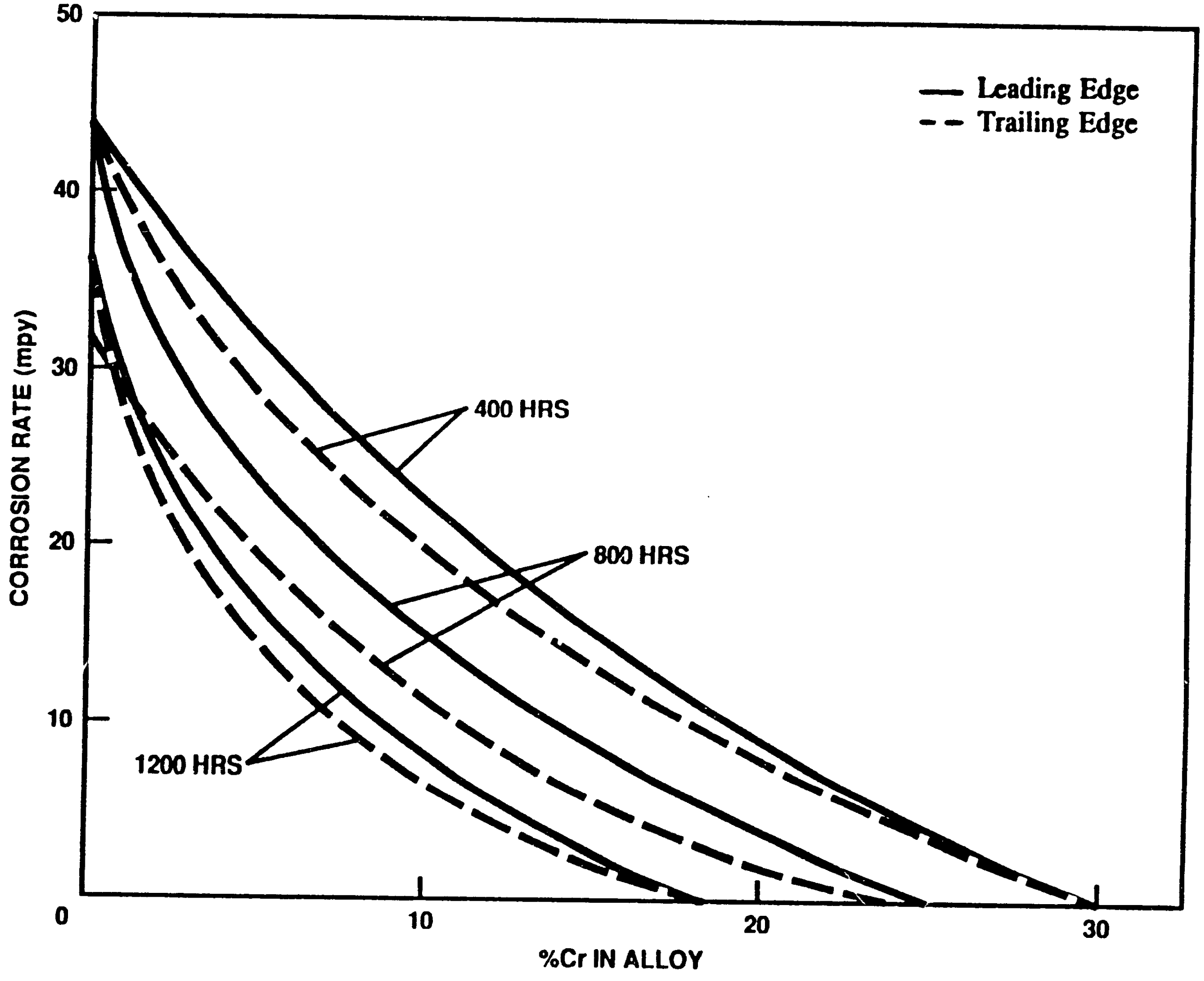

Figure 4.4. Average corrosion rate as a function of alloy chromium content at 750-850°F

to the 1200- hour maximum exposure time. In practice, a corrosion rate of less than 10 mpy after a 1000-hour operation is acceptable. Using this information as a guide, the corrosion rate which is less than 10 mpy at 1000 hours would require a minimum of ~16% Cr in the alloy. This minimum Cr concentration is found in the majority of commercially available ferritic and austenitic stainless steels, as well as high-temperature coatings.

Comparison of Tables 4.4 and 4.5 indicates that the corrosion rates of the upper probe alloys after 1200 hours of operation are similar to those in the lower probe. Such findings do not agree with the results that B&W had previously reported. Bench-scale tests [3] had shown significantly higher corrosion rates under an alternating reducing/oxidizing condition relative to a constantly reducing environment. Since it is not clear at this point if either study adequately simulated the frequency of stoichiometry fluctuations, further interpretation of the results should be deferred until additional pilot or full-scale data become available.

### 4.5 Implications

It should be emphasized that an alloy upgrade is essential only for localized regions where reducing conditions and intimate contact between high $H_2S$ concentrations and tube walls exist. Furthermore, it may not be necessary to completely replace the component alloys currently being used in the boilers. Various coating techniques, such as weld-overlay and plasma spray, can be used to apply a layer of high-chromium material on the surface of existing components.

Another way to minimize metal wastage is by optimizing the burner design. Reburning burners considered for full-scale retrofits are designed with the aid of comprehensive numerical simulations and physical flow models of flow patterns and stoichiometry [8]. With adequate reburning burner flow penetration and evading wall impingement, reducing conditions can be confined to the center of the furnace to prevent tube wastage.

## 5.0 CONCLUSIONS AND RECOMMENDATIONS

### 5.1 Conclusions

Corrosion resistance of four air-cooled probes consisting of carbon steel, a low-alloy steel, a stainless steel, and a Cr/Si-coated low-alloy steel were investigated in a coal-fired furnace simulating coal reburning conditions ($H_2S$ level and stoichiometry). Tube corrosion rates were evaluated after 400, 800, and 1200 hours of exposure to combustion gases. Based on the present results, the following conditions can be made:

(1) Metal wastage of the alloy samples increases with increasing exposure time. However, the corrosion rate decreases with time.

(2) The corrosion rate also decreases rapidly with chromium concentration in the alloy.

(3) Both the carbon and low-alloy steels were more prone to corrosion attack, while the stainless steel and the high-temperature coating demonstrated satisfactory corrosion resistance.

(4) Corrosion rates of alloys with greater than 16% Cr would be less than 10 mpy in extreme environments of high pressure and temperature boilers, burning high-sulfur coals.

(5) High-Cr alloys may be applied to the surfaces of existing boiler components in the reburning zone through commercial coating processes, such as weld-overlay and plasma spray. Therefore, costly replacement of the boiler components can be avoided.

In light of the fact that the experiments were carried out at a tube temperature of 850°F (which represents the upper range), corrosion rates at lower temperatures are expected to be substantially less. Moreover, reburner design optimization can drastically reduce the intimate contact between the reducing zone products and the boiler waterwalls; thereby, minimizing the risk of corrosion.

### 5.2 Recommendations

Three areas for future research which would complement this work and lead to a better understanding of the tube corrosion mechanisms in fossil fuel-fired boilers are suggested below:

- Scanning Electron Microscope (SEM) measurements can help to gain more insight to corrosion morphology by identifying the products formed on tube surfaces.
- Elemental dot-mapping of Fe, Cr, O, S, and other significant species would be useful in assessing the compositional distribution of the corrosion products.
- Field data are needed to determine $H_2S$ levels near boiler walls, and to further resolve the issue of corrosion in oxidizing/reducing boundaries.

As stated earlier, sixteen of the recovered tube segments were used for corrosion evaluation. Those samples have been preserved for future metallurgical analysis.

## 6.0 ACKNOWLEDGMENTS

The authors are very thankful to David Miller and Don Martin of the Materials Performance Section for test setup, instrument calibration, trouble shooting, data recording, and facility operation. Thanks are also due to Dr. Ken Ho of CRSC for many informative discussions and continued interest in this program. This work has been sponsored by the Illinois Department of Energy and Natural Resources through its Coal Development Board and Center for Research on Sulfur in Coal, and the Energy Services Division of Babcock and Wilcox.

## 7.0 REFERENCES

1. Farzan, H., Mathematical and Experimental Pilot-Scale Study of Coal Reburning for $NO_x$ Control in Cyclone Boilers, B&W Topical Report RDD:91:4576-01-02:01, Prepared for the U.S. Department of Energy, Office of Fossil Energy, Pittsburgh Energy Technology Center, July 1991.

2. S. C. Kung and L. D. Paul, "Corrosion of Waterwall Tube Materials in Low $NO_x$ Combustion Systems," **Corrosion/91**, Paper #65, 1991.

3. S. F. Chou and P. L. Daniel, "Corrosion in Low $NO_x$ Staged Combustion Units - A Literature Review," B&W Letter Report, LR:81:2877-01:01, 1981.

4. S. F. Chou, L. P. Daniel, A. J. Blazewicz, and R. F. Dudek, "Hydrogen Sulfide Corrosion in Low-$NO_x$ Combustion System," presented to AIME Annual Meeting, Detroit, MI, Sept. 17-19, 1984.

5. Detector Tube Handbook, Issued by: Drägerwerk AG Lübeck, 6th Edition, May 1985.

6. S. C. Kung and V. Srinivasan "The Effect of Yttrium on Scale Formation and Breakdown of Fe-Cr-Al in Mixed Gas," **Oxid. Met.**, Vol. 33, Nos. 5/6, 1990.

7. M. G. Fontana and N. D. Greene, **Corrosion Engineering**, McGraw-Hill Book Co., New York, 1967.

8. Farzan, H., Wessel, R. A., Sarv, H., Kir R. K., Rodgers, L. W., Maringo, G. J., and Yagiela, A. S., "Reburning Scale-up Methodology for $NO_x$ Control From Cyclone Boilers," to be presented at the ASME (IJPGC) Conference, San Diego, CA, October 1991.

# PROJECT MANAGEMENT REPORT

June 1, 1991 thru August 31, 1991

Project Title: **CYCLONE REBURNING RETROFIT: CORROSION EVALUATION**

| | |
|---|---|
| Principal Investigator: | Dr. Hamid Sarv, Babcock & Wilcox |
| Other Investigator: | Larry D. Paul, Babcock & Wilcox |
| Project Monitor: | Dr. Ken Ho, CRSC |

## COMMENTS

### Contractual Agreement

Subgrant Agreement No. CRSC 90-03 was signed and accepted by both parties on March 21, 1991. This project, "Cyclone Reburning Retrofit: Corrosion Evaluation", Project Reference No. 90-1/3.2A-1P is a part of that Agreement.

### Costs

The total project cost is estimated to be $111,318. The CRSC contract share of that estimated cost is $93,772, with Babcock & Wilcox cost sharing all remaining costs over $93,772.

### Schedule

The original project schedule was twelve (12) months. As a result of the delay in signing the Subgrant Agreement and the late start on the project tasks, a total schedule of ten (10) months is shown on page 3.

(This project is funded by the U. S. Department of Energy as part of its cost-shared program with Illinois Department of Energy and Natural Resources.)

# Projected and Estimated Expenditures by Quarter

| Quarter* | Types of Cost | Direct Labor | Materials & Supplies | Travel | Major Equipment | Other Direct Costs | Indirect Cost | Total |
|---|---|---|---|---|---|---|---|---|
| Sept. 1, 1990 to Nov. 30, 1990 | Projected | 2,208 | 4,184 | 0 | 0 | 0 | 6,218 | 12,610 |
| | Estimated | 426 | 0 | 0 | 0 | 0 | 1,074 | 1,500 |
| Sept. 1, 1990 to Feb. 28, 1991 | Projected | 16,100 | 4,184 | 0 | 0 | 0 | 41,133 | 61,417 |
| | Estimated | 5,273 | 321 | 0 | 0 | 0 | 13,353 | 18,947 |
| Sept. 1, 1990 to May 31, 1991 | Projected | 27,854 | 5,252 | 2,470 | 0 | 0 | 71,177 | 106,753 |
| | Estimated | 20,241 | 11,586 | 0 | 0 | 0 | 52,683 | 84,510 |
| Sept. 1, 1990 to Aug. 31, 1991 | Projected | 29,154 | 5,252 | 2,470 | 0 | 0 | 74,442 | 111,318 |
| | Estimated | 26,752 | 12,984 | 286 | 0 | 0 | 70,181 | 110,203** |

*Cumulative by quarter

**CRSC Share = $93,772

# COSTS BY QUARTER

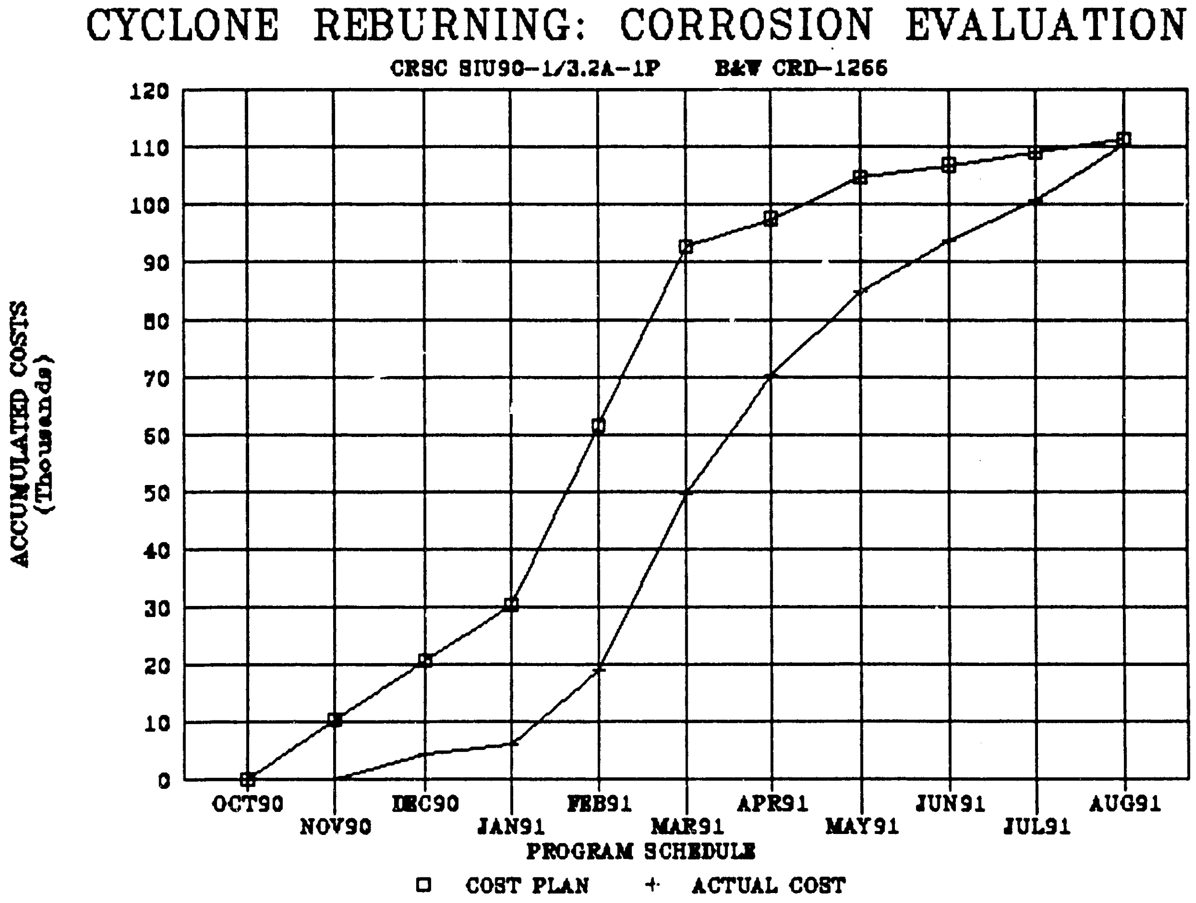

Total CRSC Award $93,772

DATE
FILMED
02 1 11 192

I